Available online at www.sciencedirect.com
ScienceDirect
Pattern Recognition Letters 28 (2007) 1240–1249
Pattern Recognition Letters
www.elsevier.com/locate/patrec

# Texture image retrieval using rotated wavelet filters

Manesh Kokare *, P.K. Biswas, B.N. Chatterji

*Department of Electronics and Electrical Communication Engineering, Indian Institute of Technology, Kharagpur 721 302 (WB), India*

Received 3 January 2005; received in revised form 10 August 2006
Available online 21 February 2007

Communicated by R. Manmatha

**Abstract**

A novel approach for texture image retrieval is proposed by using a new set of two-dimensional (2-D) rotated wavelet filters (RWF) and discrete wavelet transform (DWT) jointly. A new set of 2-D rotated wavelet improves characterization of diagonally oriented textures. Experimental results indicate that the proposed method improves retrieval rate from 70.09% to 78.44% on database D1, and from 75.62% to 80.78% on database D2, compared with the traditional DWT based approach. The proposed method also retains comparable levels of computational complexity.


*Keywords:* Content based image retrieval; Rotated wavelet filters; Canberra distance metric; Similarity measurement; Texture retrieval; Wavelets

## 1. Introduction

### 1.1. Motivation

With the rapid expansion of worldwide network and advances in information technology there is an explosive growth of multimedia databases and digital libraries. This demands an effective tool that allow users to search and browse efficiently through such a large collections. In many areas of commerce, government, academia, hospitals, entertainment, and crime preventions large collections of digital images are being created. Usually, the only way of searching these collections was by using keyword indexing, or simply by browsing. However, as the databases grew larger, people realized that the traditional keywords based methods to retrieve a particular image in such a large collection are inefficient. To describe the images with keywords with a satisfying degree of concreteness and detail, we need a very large and sophisticated keyword system containing typically several hundreds of different keywords. One of the serious drawbacks of this approach is the need of trained personnel not only to attach keywords to each image (which may take several minutes for one single image) but also to retrieve images by selecting keywords, as we usually need to know all keywords to choose good ones. Further, such a keyword based approach is mostly influenced by subjective decision about image content and also it is very difficult to change a keyword based system afterwards. Therefore, new techniques are needed to overcome these limitations. Digital image databases however, open the way to content based searching. It is common phrase that an image speaks thousands of words. So instead of manual annotation by text based keywords, images should be indexed by their own visual contents, such as color, texture and shape. The main advantage of this method is its ability to support the visual queries. Hence researchers turned attention to content based image retrieval (CBIR) methods. The challenge in image retrieval is to find out features that capture the important characteristics of an image, which make it

* Corresponding author. Address: Department of Electronics and Telecommunication Engineering, S.G.G.S. Institute of Engineering and Technology, Vishnupuri, Nanded 431 602 (Maharashtra), India. Tel.: +91 2462 268699 (residence); +91 2462 229306x220 (office); fax: +91 2462 229236.

*E-mail addresses:* mbk@ece.iitkgp.ernet.in, mbkokare@sggs.ac.in, mbkokare@yahoo.com (M. Kokare), pkb@ece.iitkgp.ernet.in (P.K. Biswas), bnc@ece.iitkgp.ernet.in (B.N. Chatterji).

0167-8655/$ - see front matter © 2007 Elsevier B.V. All rights reserved.
doi:10.1016/j.patrec.2007.02.006

unique, and allow its accurate identification. Rui and Huang (1999), Smeulders et al. (2000) and Kokare et al. (2002a) had presented comprehensive and recent extensive literature survey on content based image retrieval.

Search techniques can be based on many features such as texture, colour and shape. But the texture features are of the highest importance in computer vision because many natural scenes can be viewed as a composition of different textures. Therefore in this paper we have concentrated only on the problem of finding good texture features for CBIR.

### 1.2. Related works

The texture features currently in use are mainly derived from multi-scale approach. Liu and Picard (1996) have used Wold features for image modeling and retrieval. Manjunath and Ma (1996) have used features derived from the Gabor wavelet coefficients for indexing photographic and satellite images. In SaFe project, Smith and Chang (1998) used discrete wavelet transform (DWT) based features for image retrieval. Recently, Do and Vetterli (2002) proposed wavelet based texture retrieval using generalized Gaussian density and Kullback–Leibler distance metric. Several authors have also proposed rotation invariant texture features. Fountain et al. (1998) have given a comparative study of rotation invariant texture analysis methods. Chen and Kundu (1994) modeled the features of wavelet subband as hidden Markov model (HMM) to obtain rotation invariant features. These models are trained using texture samples belonging to the same class but with different orientations. Kashyap and Khotanzed (1986) developed a circular simultaneous autoregressive model for the extraction of rotation invariant texture features. Haley and Manjunath (1999) proposed a method of obtaining rotation invariant features by using magnitude of discrete Fourier transform of features obtained via multiresolution filter. Porter and Canagarajah (1997) proposed a pyramidal wavelet based approach for extraction of rotation invariant texture features. However, in this paper we have limited our study of texture image retrieval without rotation invariant property.

Manjunath and Ma (1996) have done extensive experiments on a large set of textured images and shown that the retrieval performance using the Gabor wavelet is better than using conventional orthogonal wavelet based features. Even though the Gabor wavelet based method give better retrieval performance, but it suffers from following three main disadvantages.

(a) Gabor functions do not form an orthogonal basis set and hence the representation is not compact, which requires more memory during computation.
(b) No efficient algorithm exists for computing the forward and inverse transformations.
(c) Computational time required for feature extraction is quite high, which limits the retrieval speed.

Recent development in wavelet theory has provided a promising alternative through multichannel filter banks that overcomes these problems. Furthermore, as wavelets form the core technology in the next generation of still image coding standard, JPEG-2000, the choice of wavelet features enables the implementation of the retrieval system that can work directly on the compressed domain. In literature, Chang and Kuo (1993), Laine and Fan (1993), Unser (1995) and Wouwer et al. (1999) have reported studies on successful application of multichannel texture analysis. All these studies revealed that the scale-frequency approach is very effective for the description and analysis of the natural textures.

In the standard wavelet decomposition, HH subband contains diagonal information. It contains directional information in two directions simultaneously both in 45° and 135°. In texture retrieval application, characterization of specific directional information of an image improves retrieval performance. That is made possible using non-separable oriented wavelet transforms, such as the hexagonal wavelet transform proposed by Simoncelli and Adelson (1990) and the steerable wavelet filters proposed by Freeman and Adelson (1991). The hexagonal wavelet representation partitions the orientations into three bands of 60° covering a frequency domain using a hexagonal sampling system and filters at the expense of implementation difficulty. Steerable filters are overcomplete. Hence in this work we have used rotated discrete wavelet filters that are obtained by rotating the standard 2-D DWT filters. Computational complexity associated with the rotated wavelet filters decomposition is same as that of the standard 2-D wavelet filters decomposition, if both are implemented in 2-D frequency domain.

### 1.3. Main contributions

First, in this work for better dealing with texture images we present a new set of 2-D rotated wavelet filters, which is designed by using Daubechies eight tap coefficients. Second, for the RWF+DWT to be used effectively in the image retrieval applications, we present the retrieval results of each individual method obtained using the traditional normalized Euclidean distance metric and combination of RWF and DWT with the Canberra distance metric. Third, for large-scale evaluation our retrieval results are checked on two different sets of large databases and compared with existing available methods on corresponding databases. Performance of the proposed method is better than that of the existing available methods both in terms of retrieval accuracy and retrieval time consistently on both the databases. Finally, a method to reduce redundancy in features obtained by using combination of RWF and DWT for texture image retrieval is also suggested.

This paper is organized as follows. In Section 2, rotated wavelet filters for CBIR is discussed in brief. The proposed image retrieval procedure is given in Section 3.

Experimental results are given in Section 4, which is followed by the conclusion in Section 5.

## 2. Rotated wavelet filters for CBIR

Rourke and Stevenson (1995) have used diamond shaped wavelet filters for image compression. They have shown that this technique incorporates some of the properties of human visual system. Kim and Udpa (2000) have designed rotated wavelet filters using Haar wavelet filters for texture classification. Though the Haar wavelet transform has a number of advantages such as conceptually simple, fast and memory efficient, but it has certain limitations, which can be a problem for some applications like capturing high frequency information in an image such as edges. In generating each set of averages for the next level and each set of detail coefficients, the Haar transform performs an average and difference on a pair of values. Then the algorithm shifts over by two values and calculates another average and difference on the next pair. The high frequency coefficient spectrum should reflect all high frequency changes. The Haar window is only two elements wide. If a big change takes place from an odd pixel location to an even pixel location, the change will not be reflected in the high frequency coefficients. Edge information is a very important feature in texture images. The wavelet developed by Daubechies (1992) retains edge information by using overlapping windows. This motivates us to use Daubechies wavelet coefficients for designing rotated wavelet filters. Here we have designed a new set of rotated wavelet filters using Daubechies eight tap filter coefficients. We have demonstrated the effectiveness of use of the RWF in addition to the standard DWT for extracting texture features in CBIR.

### 2.1. Separable wavelets

The wavelet basis functions are constructed by the dyadic dilation and translation of the mother wavelet $\psi_{i,l} = 2^{-i/2}\psi\left(\frac{x}{2^i} - l\right)$, where $i$ and $l$ are the scale and translation indices, respectively. The coefficient of lowpass filter $h$ and high pass filter $g$ can be selected such that $\{\psi_{i,l}\}_{i,l\in z^2}$ constitutes an orthonormal basis of $L_2$. Then, the wavelet coefficients $d_i$ and the approximation coefficients $s_i$ of a function $f(x)$ at scale $i$ can be obtained by

$$d_i(l) = \langle f(k), \psi_{i,l}(k)\rangle, \quad s_i(l) = \langle f(k), \phi_{i,l}(k)\rangle \tag{1}$$

where $\langle\cdot\rangle$ denote the standard $L_2$ inner product and $\phi_{i,l}(k)$ is the discrete scaling function at resolution $i$. In order to generate a multi-scale pyramid representation, the transform is applied recursively to the approximate coefficients $s_i$ resulting in $s_{i+1}$ and $d_{i+1}$. Finally, one can obtain the full discrete wavelet synthesis of a function $f(x)$ by combining the coefficients over all scales down to the given depth $I$

$$f(x) = \sum_{l\in z} s_I(l)\phi_{I,l} + \sum_{i=1}^{I}\sum_{l\in z} d_i(l)\psi_{i,l} \tag{2}$$

where $s_I$ represents the coefficients of the coarser signal approximation $f_I(x)$. The separable wavelet transform proposed by Mallat (1989) is the most common method for extending the one-dimensional wavelet transform to two-dimension. Filtering is performed at each level first along one dimension and then in the other dimension.

### 2.2. 2-D wavelets

Although the separable wavelet transform is widely used, the non-separable 2-D DWT can be computed by filtering a given image $f(x,y)$ with 2-D wavelet filters followed by 2-D downsampling operations as illustrated in Fig. 1. 2-D wavelet filters can be obtained from the products of one-dimensional wavelet and scaling functions. One can construct a 2-D scaling and three 2-D wavelet functions as

$$\begin{aligned} \phi(i,j) &= \phi(i)\phi(j), \quad \psi_1(i,j) = \phi(i)\psi(j) \\ \psi_2(i,j) &= \psi(i)\phi(j), \quad \psi_3(i,j) = \psi(i)\psi(j) \end{aligned} \tag{3}$$

The 2-D filters $H_{ll}$, $H_{lh}$, $H_{hl}$ and $H_{hh}$ shown in Fig. 1 are obtained from Eq. (3) and they correspond to $\phi$, $\psi_1$, $\psi_2$ and

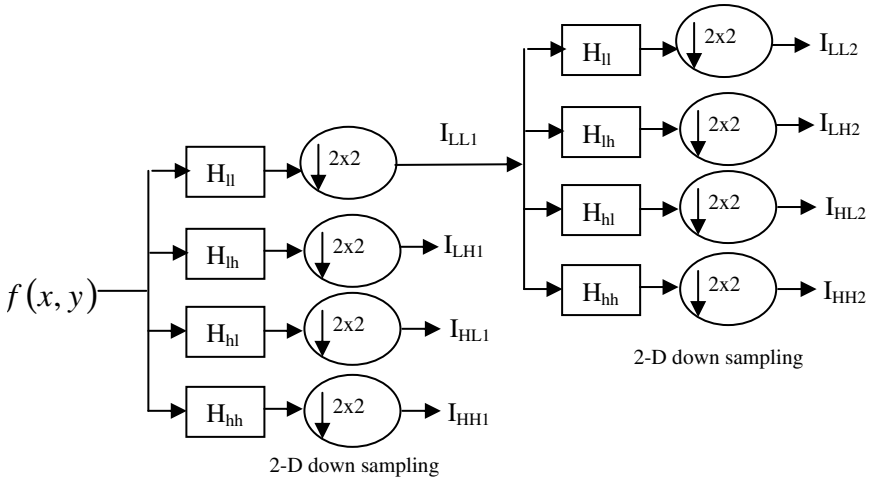


Fig. 1. Filter bank structure of a two level 2-D DWT decomposition using 2-D wavelet filters.

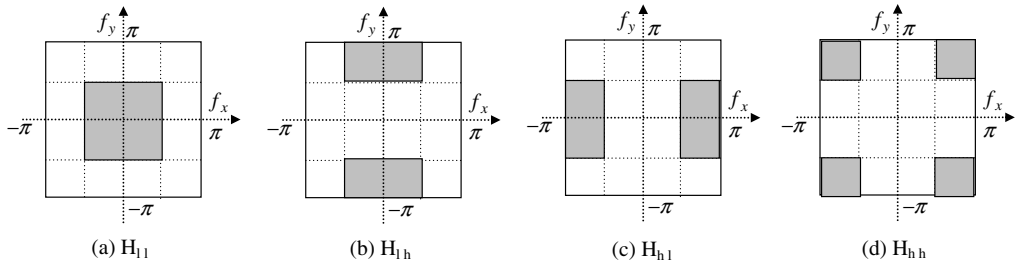


Fig. 2. Frequency domain partition resulting from the one level DWT decomposition.

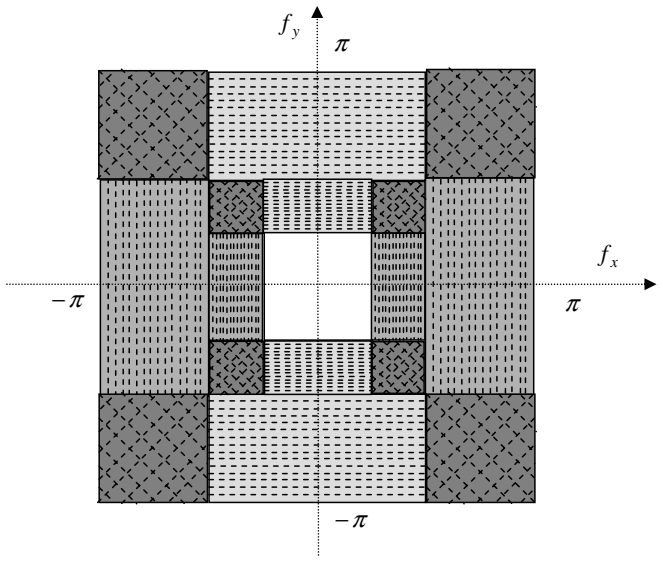


Fig. 3. Frequency domain partition resulting from two levels of DWT decomposition.

$\psi_3$ respectively. Although 2-D approach involves more operations than 1-D filtering approach, this method can be very efficiently implemented in the parallel processing environment. The frequency partition for one and two level 2-D wavelet transform decomposition is illustrated in Figs. 2 and 3 respectively.

### 2.3. Rotated wavelet filter

$I_{HH}$ subband in the standard DWT decomposition contains the diagonal information of textured image. It is difficult to distinguish, whether that the diagonal information is oriented in 45° or 135°. In texture retrieval application, in many cases, characterization of specific directional information of an image improves retrieval performance. This is also supported by our experimental results given in Section 4. Non-separable oriented wavelet transform obtained with the rotated wavelet filters characterizes texture in specific directions. For designing the 2-D rotated wavelet filters, Daubechies eight tap filter coefficients are used. Rotated wavelet filter sets are obtained by rotating the standard 2-D discrete wavelet filters by 45° so that the decomposition is performed along the new directions $f_x'$ and $f_y'$ as shown in Fig. 5, which are 45° apart from decomposition directions of the standard DWT. Let $h$ and $g$ represent the one-dimensional Daubechies eight tap wavelet low pass and high pass filter coefficients respectively.

$$h = \begin{bmatrix} 0.23037781330886 & 0.71484657055254 & 0.63088076792959 & -0.02798376941698 \\ -0.18703481171888 & 0.03084138183599 & 0.03288301166698 & -0.01059740178500 \end{bmatrix}$$

$$g = \begin{bmatrix} 0.01059740178500 & 0.03288301166698 & 0.03084138183599 & -0.18703481171888 \\ 0.02798376941698 & 0.63088076792959 & -0.71484657055254 & 0.23037781330886 \end{bmatrix}$$

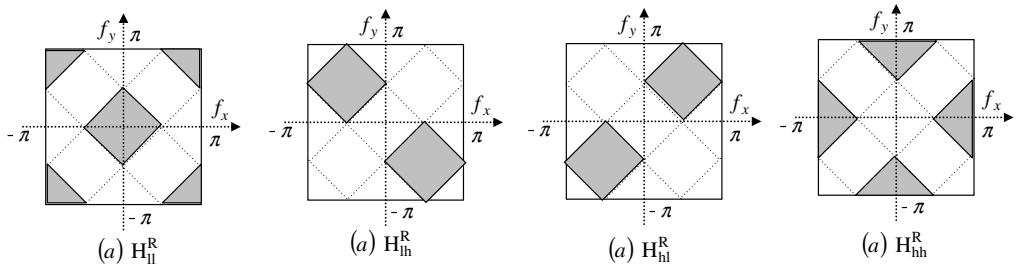


Fig. 4. Frequency domain partition resulting from one level RWF.

The 2-D low–low, low–high, high–low, and high–high filter coefficients are derived from $h$ and $g$ using the following matrix operations.

$$\begin{aligned} H_{\mathrm{LL}} &= h^{\mathrm{T}}h \\ H_{\mathrm{LH}} &= h^{\mathrm{T}}g \\ H_{\mathrm{HL}} &= g^{\mathrm{T}}h \\ H_{\mathrm{HH}} &= g^{\mathrm{T}}g \end{aligned} \tag{4}$$

The rotated 2-D wavelet filter coefficients $H_j^{\mathrm{R}}$ are obtained by rotating the corresponding 2-D wavelet filter coefficient $H_j$ by 45° (where $j$ denotes LL, LH, HL, or HH). The size of a filter is $(2N-1)\times(2N-1)$, where $N$ is the length of the 1-D filter. The computational complexity associated with the RWF decomposition is same as that of the standard 2-D DWT, if both are implemented in the 2-D frequency domain. Partitions in frequency domain resulting from one and two level RWF decomposition is shown in Figs. 4 and 5 respectively. Each subband covers a quarter of whole frequency region and the set of RWF's retains the orthogonality property, because the following condition holds:

$$\frac{1}{2\pi}\int_{-\infty}^{\infty} S_i(\omega)\overline{S_j(\omega)}\mathrm{d}\omega = 0 \quad (i \neq j) \tag{5}$$

where $S_i(\omega)$ is the Fourier transform of the 2-D filters $H_i$ and $i$ denotes either of ll, lh, hl or hh. With rotated wavelet decomposition the diagonal characteristics in 45° and 135° orientations are obtained in $I_{\mathrm{LH}}^{\mathrm{R}}$ and $I_{\mathrm{HL}}^{\mathrm{R}}$ subbands respectively. This characteristic of the RWF sets provides important complementary information to the standard DWT filter set for extracting texture features for content based image retrieval. An example of one level image decomposition using standard DWT and RWF is shown in Fig. 6a and b respectively. Texture characteristics oriented in 45° and 135° are clearly seen in the subband $I_{\mathrm{LH}}^{\mathrm{R}}$ and $I_{\mathrm{HL}}^{\mathrm{R}}$ respectively.

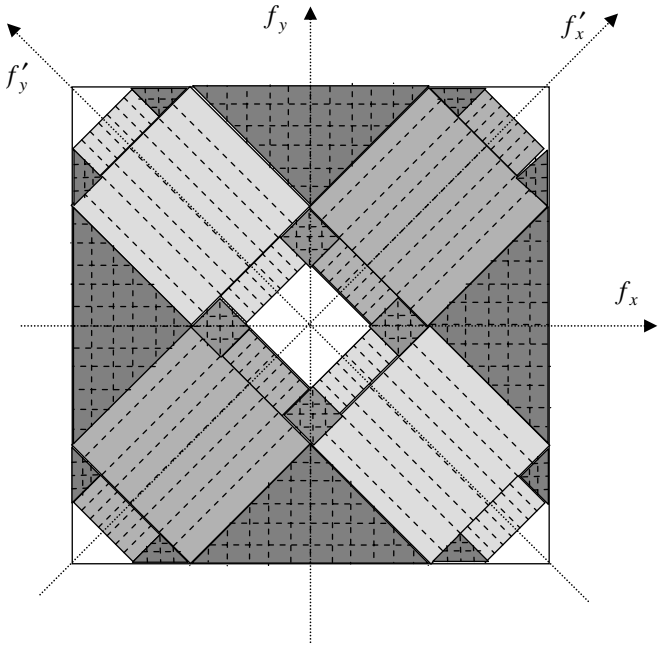


Fig. 5. Frequency domain partition resulting from two levels RWF.

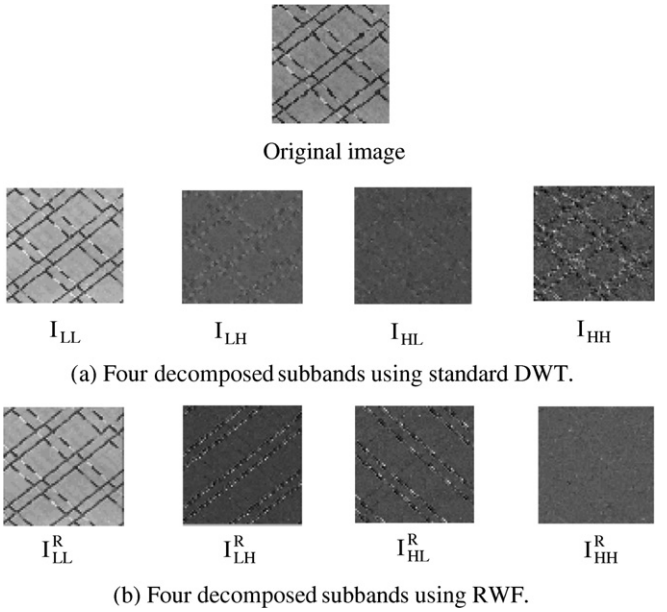


Fig. 6. One level wavelet decomposition of texture image D47 using (a) standard DWT and (b) RWF.

## 3. Texture image retrieval

In this section texture image database used for experimental purpose, texture features and image retrieval method are discussed.

### 3.1. Texture image database

#### 3.1.1. Database D1

The texture database D1 used in our experiment consists of 116 different textures. We have used 108 textures from Brodatz texture photographic album (1966), seven textures from USC (University of Southern California) database and one artificial texture. Size of each texture image is $512\times512$. Each $512\times512$ image is divided into sixteen $128\times128$ non-overlapping subimages, thus creating a database of 1856 texture images.

#### 3.1.2. Database D2

This database consists of 40 textures obtained from MIT Vision Texture (VisTex) database. These are real world $512\times512$ images from different natural scenes. Only gray-scale levels of the images (computed from the luminance component) were used in the experiments. Since we define similar texture images from a single original one, we have selected texture images whose visual properties do not change too much over the image. Each $512\times512$ image is divided into sixteen $128\times128$ non-overlapping subimages, thus creating a database of 640 texture images.

### 3.2. Texture features

Each image from database D1 and D2 is decomposed using RWF and DWT and four different sets of features are computed as follows.

(a) Feature Set1: DWT only
(b) Feature Set2: RWF only
(c) Feature Set3: RWF and DWT
(d) Feature Set4: ($I_{LH}$ and $I_{HL}$ components of RWF) and DWT.

The analysis was performed up to fifth level of decomposition. In each set, feature vector is formed using energy and standard deviation of every subband. The basic assumption of using energy as a feature for texture discrimination is that the energy distribution in the frequency domain identifies a texture. Besides providing acceptable retrieval performance from large texture database, energy based approach is partly supported by physiological studies of the visual cortex, which was presented by Hubel and Wiesel (1962) and Daugman (1980). Manjunath and Ma (1996) and Kokare et al. (2002a,b, 2003a,b, 2004) have shown that the retrieval performance with combination of these two feature parameters was always found to be better than that of using these features individually. The Energy and Standard Deviation of wavelet subband are computed as follows.

$$\text{Energy} = \frac{1}{M \times N} \sum_{i=1}^{M} \sum_{j=1}^{N} |X_{ij}| \tag{6}$$

$$\text{Standard deviation} = \left[ \frac{1}{M \times N} \sum_{i=1}^{N} \sum_{j=1}^{M} (X_{ij} - \mu_{ij})^2 \right]^{\frac{1}{2}} \tag{7}$$

where $M \times N$ is the size of wavelet subband, $X_{ij}$ is wavelet coefficient, and $\mu_{ij}$ is the mean value of wavelet coefficient. Length of the feature vector is equal to (*No. of subbands* × *No. of feature parameters used in combination*) elements. For creation of the feature database above procedure is repeated for all the images of the image database and these feature vectors are stored in the feature database.

### 3.3. Image retrieval method

A query pattern is any one of the patterns from image database. This pattern is processed to compute the feature vector in the same manner as discussed in Section 3.2. A distance metric is used to compute the similarity between two images. If $x$ and $y$ are two $d$-dimensional feature vectors of the database image and the query image respectively, then the Euclidean distance is defined as

$$d_E(x,y) = \sqrt{\sum_{i=1}^{d} (x_i - y_i)^2} \tag{8}$$

Euclidean distance is not always the best metric. The fact is that the distances in each dimension are squared before summation, places great emphasis on those features for which the dissimilarity is large. Hence it is necessary to normalize the individual feature components before finding the distance between two images. This has been taken care of in Canberra distance metric, which motivates us to use Canberra distance metric as dissimilarity measure. This is also supported by our experimental results given in Table 1. Canberra distance is given by

$$\text{Canb}(x,y) = \sum_{i=1}^{d} \frac{|x_i - y_i|}{|x_i| + |y_i|} \tag{9}$$

In Eq. (9), the numerator signifies the difference and denominator normalizes the difference. Thus distance value will never exceed one, being equal to one whenever either of the attributes is zero. Thus it appears to be a good similarity measure to be used, which avoids scaling effect. Kokare et al. (2003a,b) have reported that retrieval accuracy not only depends on strong set of features, but also on good similarity measure. Manjunath and Ma (1996) used the normalized Euclidean distance metric as a similarity measure, which is given by

$$\text{NED}(x,y) = \sum_{m} \sum_{n} d_{mn}(x,y),$$

where

$$d_{mn}(x,y) = \left| \frac{\mu^x_{mn} - \mu^y_{mn}}{\sigma(\mu_{mn})} \right| + \left| \frac{\sigma^x_{mn} - \sigma^y_{mn}}{\sigma(\sigma_{mn})} \right| \tag{10}$$

where $m$ and $n$ are scale and orientation resulting from wavelet decomposition, $\mu_{mn}$ and $\sigma_{mn}$ are the mean and the standard deviation of the magnitude of the wavelet decomposed subband that are used as features of the image, $\sigma(\mu_{mn})$ and $\sigma(\sigma_{mn})$ are the standard deviations of the respective features over the entire database and are used to normalize the individual feature components.

Table 1
Average retrieval accuracy of 116 texture images of the database D1 with different feature measures

| Level of decomposition | Feature measure | Standard DWT (%) | RWF (%) | DWT + RWF (%) | DWT + ($I_{LH}$ and $I_{HL}$) subbands of RWF (%) |
|---|---|---|---|---|---|
| 1 | Energy | 53.71 | 47.91 | 56.78 | 54.74 |
| | Standard deviation | 51.56 | 50.05 | 64.22 | 58.94 |
| | Energy + standard deviation | 59.80 | 54.74 | 64.49 | 63.57 |

Normalized Euclidean distance metric is used as a similarity measure for feature sets 1 and 2, while the Canberra distance metric is used for feature sets 3 and 4. It is obvious that the distance of an image from itself is zero. The distance vector is stored in increasing order and the closest sets of patterns are retrieved. In the ideal case all the top 16 retrievals are from the same large image. The performance is measured in terms of the average retrieval rate, which is defined as the average percentage number of patterns belonging to the same image as the query pattern in the top 16 matches.

## 4. Experimental results

We have conducted two different sets of experiments using different databases and different feature measures to test the retrieval performance. In the first set of experiments, database D1 is used. The same database was also used by Manjunath and Ma (1996) and reported Gabor wavelet based texture image retrieval results using four scales and six orientations. For constructing feature vector they used mean and standard deviation of the magnitude of the Gabor transform coefficients, resulting in a feature vector of size $24 \times 2$. The results of the proposed method are compared with existing Gabor wavelet based method.

In second series of experiments, database D2 is used. Features are extracted using feature sets 1–4. The same database was also used by Do and Vetterli (2002) and proposed wavelet based texture image retrieval using generalized Guassian density and Kullback–Leibler distance (GGD & KLD) method. In this experiment the results of the proposed method are compared with GGD & KLD based method.

### 4.1. Average retrieval accuracy

Table 1 presents a detailed comparison of the average retrieval accuracy for 116 different textures from database D1 using feature sets 1–4. Table 2 provides a comparison of average retrieval accuracy for the database D1 with different level of wavelet decomposition. Table 3 provides a comparison of average retrieval accuracy for 40 different textures from the database D2 using feature sets 1–4, and GGD & KLD. Following are the main observations.

(1) First, from Table 1 it is observed that the combination of standard deviation and energy as a feature measure always outperforms the individual feature measures.
(2) Secondly, the proposed method (DWT + RWF) consistently outperforms the other methods on both the databases. The main reason is that RWF provides complementary texture information to the DWT by making use of its orientation selectivity. Also combination of DWT and RWF features is more expressive in characterizing textures than the DWT based ones.

Table 2
Average retrieval accuracy of 116 texture images of the database D1 with Energy + Standard deviation as a feature measure and different levels of wavelet decomposition

| Levels of decomposition | Standard DWT (%) | RWF (%) | DWT + RWF (%) | DWT + (ILH and IHL) subbands of RWF (%) | Gabor wavelet based method proposed by Manjunath and Ma (1996) (%) |
|---|---|---|---|---|---|
| 1 | 59.80 | 54.74 | 64.49 | 63.57 | 74.32 |
| 2 | 67.45 | 60.93 | 71.82 | 69.39 | |
| 3 | 69.61 | 61.74 | 75.80 | 76.02 | |
| 4 | 70.25 | 61.15 | 78.09 | 77.80 | |
| 5 | 70.09 | 57.48 | 78.44 | 77.90 | |

Table 3
Average retrieval accuracy of 40 texture images of the database D2 with Energy + Standard deviation as feature measure and fifth level of wavelet decomposition

| Level of decomposition | Standard DWT | RWF | DWT + RWF | DWT + ($I_{LH}$ and $I_{HL}$) subbands of RWF | GGD & KLD based method proposed by Do and Vetterli (2002) |
|---|---|---|---|---|---|
| 5 | 75.62% | 67.81% | 80.46% | 80.78% | 76.57% |

Table 4
Feature vector length, feature extraction and searching time of query image

| Feature measure | Standard DWT | RWF | DWT + RWF | DWT + ($I_{LH}$ and $I_{HL}$) subbands of RWF | Gabor wavelet | GGD KLD |
|---|---|---|---|---|---|---|
| Feature vector length | 40 ($20 \times 2$) | 40 ($20 \times 2$) | 80 ($40 \times 2$) | 60 ($30 \times 2$) | 48 ($24 \times 2$) | 18 ($9 \times 2$) |
| Feature extraction time (s) | 0.328 | 0.469 | 0.787 | 0.654 | 3.48 | 0.378 |
| Searching and sorting time (s) | 0.06 | 0.06 | 0.086 | 0.086 | 0.06 | 0.05 |

(3) Features using ($I_{LH}$ and $I_{HL}$ components of RWF) + DWT reduce the redundancy of complete DWT + RWF features. This is possible since the overlap between the filter responses of $H_{LL}$ and $H_{LL}{}^{R}$ as shown in Figs. 3 and 5, respectively is quite significant in frequency domain, which results in a lot of redundant information. Also the filter response of $H_{HH}^{R}$ is completely covered by those $H_{LH}$ and $H_{HL}$ filters. Retrieval accuracy with this feature set is 77.90% for the database D1 and 80.78% for the database D2.

(4) Finally, from Table 2 it is observed that the retrieval accuracy increases with the increase in level of wavelet decomposition. There is marginal improvement in the retrieval accuracy, when level of wavelet decomposition increases from fourth to fifth level.

### 4.2. Retrieval time

Table 4 provides CPU times for feature extraction and search of the database for given query image (on a pentium3 computer with 866 MHz) and feature vector length for the different feature sets. All the features are computed in MATLAB 5.3. In terms of feature extraction time for query image, the Gabor wavelet is most expensive. The proposed method also retains comparable levels of computational complexity. Feature extraction time for the query image using the proposed method is approximately 4.5 times less than the Gabor wavelets based method.

### 4.3. Retrieval accuracy as a function of number of top images considered

We evaluated the performance in terms of the average rate of retrieving relevant images as a function of the number of top retrieved images. Figs. 7 and 8 show graphs illustrating this comparison according to the number of top matches considered for the database D1 and D2 respectively by using Energy + Standard deviation feature. From Fig. 7, it is clear that the proposed method is superior to the standard DWT and the Gabor wavelet based method. If the top 116 (6% of the database) retrievals are considered the performance increases up to 92.45%, 85.23%, 94.34%, 94.50%, and 92.375% using feature sets 1–4 and the Gabor wavelet respectively. The proposed method always outperforms the earlier methods. This consistency is also seen in Fig. 8, when experiments were conducted on the image database D2. The proposed method outperforms the DWT and GGD & KLD based method reported by Do and Vetterli (2002).

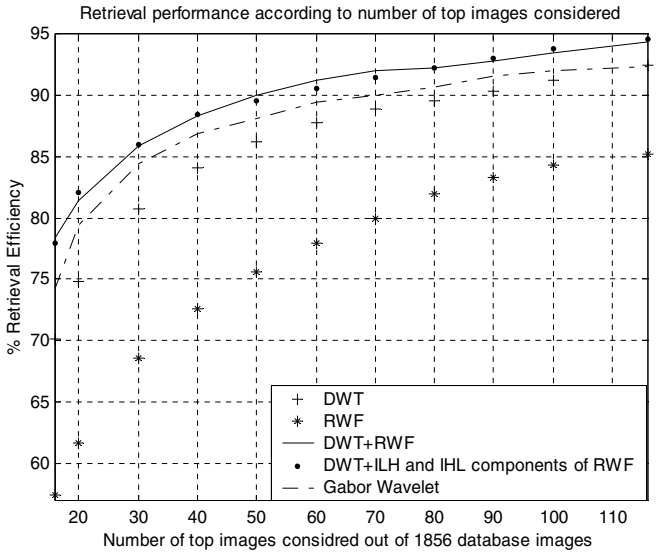


Fig. 7. Average retrieval rate of database D1 according to no. of top images.

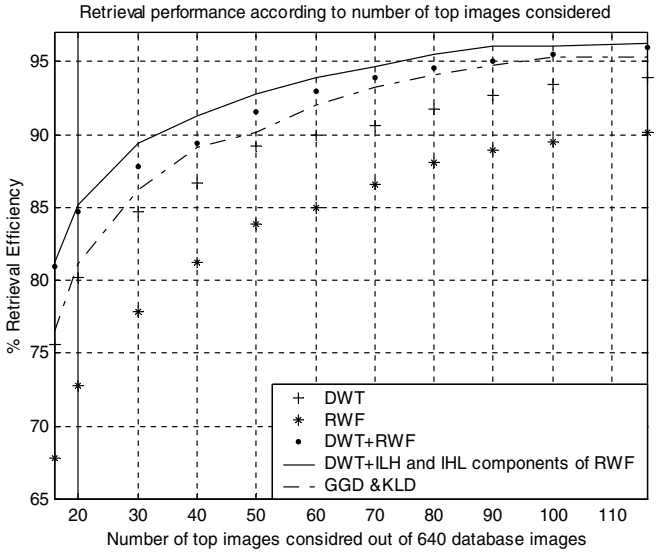


Fig. 8. Average retrieval rate of database D2 according to no. of top images considered.

### 4.4. Retrieval example

Retrieved top 20 similar images from the database D1 and D2 for a sample query image are shown in Fig. 9. Images are displayed from top left to right bottom in the increasing order of distance from query image. Examples shown are some of the difficult patterns to analyze. Retrieval example of texture image D62 from the database D1, which is randomly positioned micropatterns that lacks directionality and belongs to grainy texture class is shown in Fig. 9a. Fig. 9b shows retrieval example of texture D41 from the database D1, which is complex texture and difficult to describe. In Fig. 9c, the query image is "flower 5" from the database D2.

## 5. Conclusion

A new set of 2-D rotated wavelet is designed by using Daubechies eight tap coefficients to improve the retrieval accuracy. Two-dimensional (2-D) rotated wavelet filters

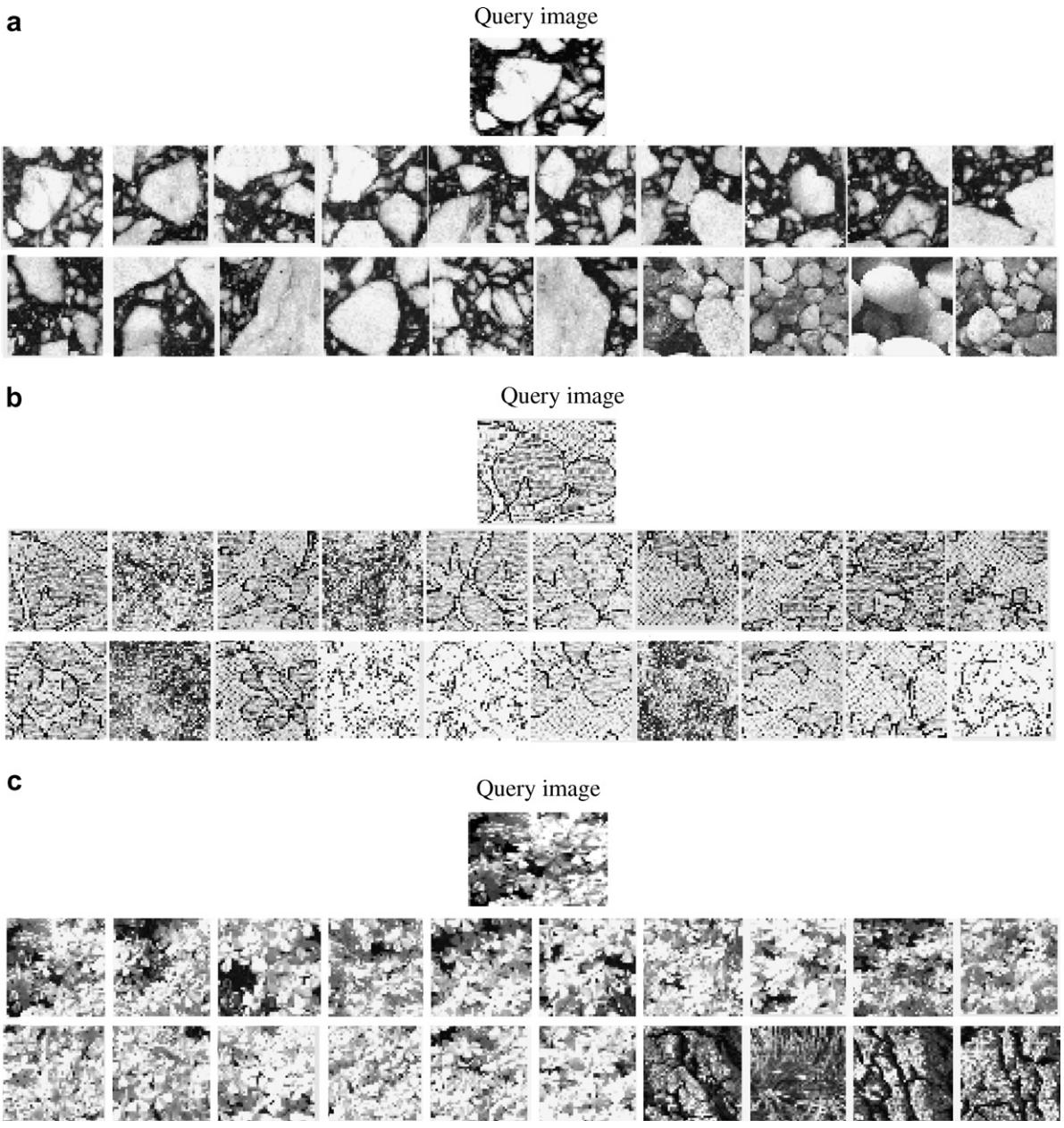


Fig. 9. Retrieved top 20 similar images for given query image. (a) D62 from database D1, (b) D41 from database D1 and (c) flowers 5 from database D2; all images are ranked in the order of similarity with the query image from left to right and top to bottom.

that are non-separable and oriented, improves characterization of diagonally oriented textures. Application of 2-D rotated wavelet filters and DWT jointly for texture image retrieval is presented. Experimental results on the database D1 consisting of 1856 texture images and the database D2 consisting of 640 texture images indicate that the proposed method significantly improves retrieval performance, e.g. from 70.09% to 78.44% on database D1 and 75.62% to 80.78% on database D2, over the traditional approach. The results of the proposed method are also compared with earlier reported methods and found that the proposed method outperforms the existing methods. Features obtained using combination of RWF and DWT are redundant. Method to reduce redundancy in these features using only ($I_{LH}$ and $I_{HL}$ components of RWF) and DWT based feature for texture image retrieval is also suggested. This method also maintains nearly equal retrieval performance as that of full RWF and DWT based features. Computational complexity of the proposed method is approximately 4.5 times less than that of the existing Gabor wavelet based method.

Further research could be focused on investigating the impact on retrieval performance for different choices of wavelet filters. Currently Daubechies eight tap coefficient filters are used for designing RWF. Designing RWF with higher tap coefficient could have given even better performance. Also the proposed method can be applied for other pattern recognition problems such as denoising or texture

segmentations. Furthermore we can extend proposed method using hidden Markov model to obtain rotation invariant texture features for content based image retrieval. This effort is currently underway and preliminary results are very encouraging.

## Acknowledgements

The authors would like to thank the anonymous reviewers for insightful comments and helpful suggestions to improve the quality, which have been incorporated in this manuscript.

## References

Brodatz, P., 1966. Textures: A Photographic Album for Artists & Designers. Dover, New York.

Chang, T., Kuo, C.C.J., 1993. Texture analysis and classification with tree-structured wavelet transform. IEEE Trans. Image Process. 2, 429–441.

Chen, J.L., Kundu, A., 1994. Rotational and gray-scale transform invariant texture identification using wavelet decomposition and hidden Markov model. IEEE Trans. Pattern Anal. Machine Intell. 16, 208–214.

Daubechies, I., 1992. Ten Lectures on Wavelets. SIAM, Philadelphia, PA.

Daugman, J., 1980. Two-dimensional spectral analysis of cortical receptive field profile. Vision Res. 20, 847–856.

Do, M.N., Vetterli, M., 2002. Wavelet-based texture retrieval using generalized Guassian density and Kullback–Leibler distance. IEEE Trans. Image Process. 11, 146–158.

Fountain, S.R., Tan, T.N., Baker, K.D., 1998. Comparative study of rotation invariant classification and retrieval of texture images. In: Proc. British Computer Vision Conf.

Freeman, W.T., Adelson, E.H., 1991. The design and use of steerable filters. IEEE Trans. Pattern Anal. Machine Intell. 13, 891–906.

Haley, G.M., Manjunath, B.S., 1999. Rotation-invariant texture classification using complete space–frequency model. IEEE Trans. Image Process. 8, 255–269.

Hubel, D.H., Wiesel, T.N., 1962. Receptive fields, binocular interaction and functional architecture in the cat's visual cortex. J. Physiol. 160, 106–154.

Kashyap, R.L., Khotanzed, A., 1986. A model-based method for rotation invariant texture classification. IEEE Trans. Pattern Anal. Machine Intell. 8, 472–481.

Kim, N.D., Udpa, S., 2000. Texture classification using rotated wavelet filters. IEEE Trans. Syst. Man Cybernet. Part A: Syst. Human 30, 847–852.

Kokare, M., Chatterji, B.N., Biswas, P.K., 2002a. A survey on current content based image retrieval methods. IETE J. Res. 48, 261–271.

Kokare, M., Chatterji, B.N., Biswas, P.K., 2002b. M-band wavelet based texture features for content based image retrieval. In: Proc. Indian Conf. on Vision, Graphics and Image Processing (ICVGIP 2002), Ahemadabad (India), pp. 173–178.

Kokare, M., Chatterji, B.N., Biswas, P.K., 2003a. Wavelet transform based texture features for content based image retrieval. In: Proc. 9th National Conf. Communications, Chennai (India), pp. 443–447.

Kokare, M., Chatterji, B.N., Biswas, P.K., 2003b. Comparison of similarity metrics for texture image retrieval. In: Proc. IEEE TENCON Conf., Bangalore (India), pp. 571–575.

Kokare, M., Chatterji, B.N., Biswas, P.K., 2004. Cosine-modulated wavelet based texture features for content based image retrieval. Pattern Recognition Lett. 25, 391–398.

Laine, A., Fan, J., 1993. Texture classification by wavelet packet signature. IEEE Trans. Pattern Anal. Machine Intell. 15, 1186–1191.

Liu, F., Picard, R.W., 1996. Periodicity, directionality, and randomness: Wold features for image modeling and retrieval. IEEE Trans. Pattern Anal. Machine Intell. 18, 722–733.

Mallat, S., 1989. A theory for multiresolution signal decomposition: The wavelet representation. IEEE Trans. Pattern Anal. Machine Intell. 11, 674–693.

Manjunath, B.S., Ma, W.Y., 1996. Texture features for browsing and retrieval of image data. IEEE Trans. Pattern Anal. Machine Intell. 8, 837–842.

Porter, R., Canagarajah, N., 1997. Robust rotation-invariant texture classification: Wavelet, Gabor filter and GMRF based schemes. IEE Proc. Vision Image Signal Process. 144, 180–188.

Rourke, T.P.O., Stevenson, R.L., 1995. Human visual system based wavelet decomposition for image compression. J. Visual Commun. Image Representation 6, 109–121.

Rui, Y., Huang, T.S., 1999. Image retrieval: Current techniques, promising directions and open issues. J. Visual Commun. Image Representation 10, 39–62.

Simoncelli, E.P., Adelson, E.H., 1990. Non-separable extensions of quadrature mirror filters to multiple dimensions. Proc. IEEE 78, 652–664 (Special issue on multi-dimensional signal processing).

Smeulders, A.W.M., Worring, M., Santini, S., Gupta, A., Jain, R., 2000. Content-based image retrieval at the end of the early years. IEEE Trans. Pattern Anal. Machine Intell. 22, 1349–1380.

Smith, J.R., Chang, S.F., 1998. VisualSeek: A fully automated content based image query system. In: Proc. of ACM Internat. Conf. Multimedia, Boston, MA, pp. 87–98.

Unser, M., 1995. Texture classification and segmentation using wavelet frames. IEEE Trans. Image Process. 4, 1549–1560.

Wouwer, G.V., Scheunders, P., Dyck, D.V., 1999. Statistical texture characterization from discrete wavelet representation. IEEE Trans. Image Process. 8, 592–598.